# Bring-Your-Own-Phantom (BYOP): A Flexible Stand-Alone Distortion Analysis Prototype

**Lumeng Cui, Ph.D.[1]; Gerald Moran, Ph.D.[2]; Niranjan Venugopal, M.Sc., Ph.D., MCCPM[3,4,5]**

[1]Research Scientist, Siemens Healthcare Limited, Oakville, Ontario, Canada
[2]Director of Research, Siemens Healthcare Limited, Oakville, Ontario, Canada
[3]Department of Medical Physics, CancerCare Manitoba, Winnipeg, Manitoba, Canada
[4]Department of Physics and Astronomy, University of Manitoba, Winnipeg, Manitoba, Canada
[5]Department of Radiology, University of Manitoba, Winnipeg, Manitoba, Canada

## Short synopsis

Magnetic Resonance Imaging (MRI) is increasingly becoming an essential component in radiation therapy (RT) planning and with it, characterization of the geometric distortion latent in MR imaging. Current methods available for performing distortion measurements are often performed as offline calculations. In this work, we have developed a prototype that can accommodate any type of grid-like phantom and provides an on-the-scanner software solution for the analysis of spatial distortion MR images. The prototype takes a prior CT scan and a newly acquired MR dataset as inputs and generates a qualitative visualization and quantitative evaluation for the spatial distortion in the MRI volume. The prototype was assessed using three grid-like phantoms with good success.

## Introduction

The characterization of distortion in MRI is not a new phenomenon. In fact, our understanding of the topic goes back almost 30 years, when MRI was being used for stereotactic radiation therapy [1–5]. In that era of radiation treatment planning, the MR image was often fused to the computed tomography (CT) image via image registration. Since the images were co-registered, the MR image was primarily used to delineate the cancer, which could not be seen on the CT image. In this scenario, the spatial fidelity of the MRI was of less importance since the CT image was the primary dataset being used to position the patient and perform the necessary dose calculations. Fast-forward 30 years, and the use of MRI for radiotherapy remains very much the same at many centers, with the MRI being used for delineation via image registration. But a lot has changed in three decades: Radiation oncology has trended toward treatments that are depositing much more radiation dose in far fewer fractions. In this new paradigm, the precision and accuracy of radiation treatments have increased. The drive for more precision targeting has led to the development of MR-only radiation treatment workflows, and systems that combine MRI and linear acceleration, known as MR-Linacs [6–8]. Because of this trend, we have seen increased attention being paid to methods of spatial distortion correction and to various ways of characterizing the residual distortion [9–13]. A lot of work has been done to understand the effect of MRI distortion for specific treatment sites [14–20].

Thus, MRI is increasingly being used in radiation therapy procedures, and measuring residual geometric distortion has become even more vital. Even though MRI can provide superior soft-tissue contrast than CT imaging, MRI suffers spatial distortion deviating from isocenter due to the nonlinearity of magnetic gradients. This spatial distortion increases with increasing distance from the isocenter. Although vendor-supplied correction algorithms can help mitigate the spatial distortion, there is still a need to monitor any potential distortion that might jeopardize the safety and accuracy of the MR imaging that is being incorporated into radiation treatment planning. In this regard, proper software and (grid-like) phantoms are indispensable for performing an accurate distortion measurement and quality-control monitoring. However, in the current marketplace, phantoms and software used for distortion measurements are often expensive and require subscriptions for software, which may hinder smaller

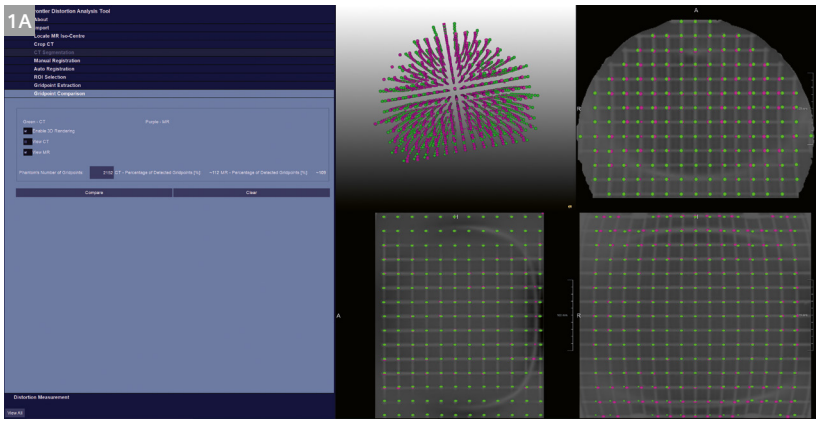


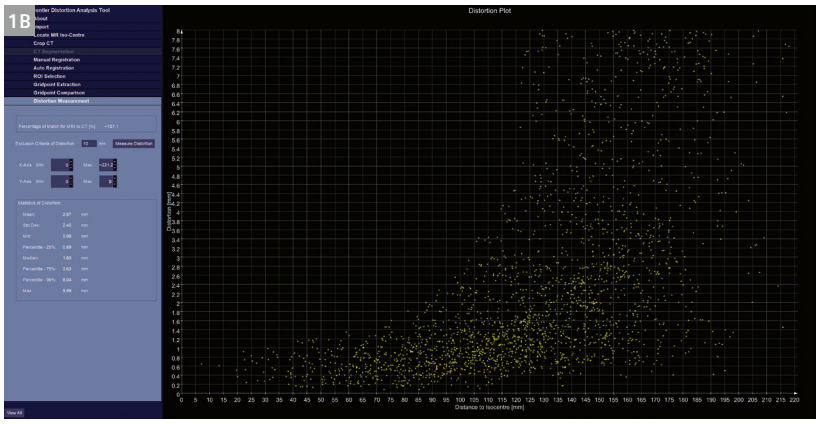



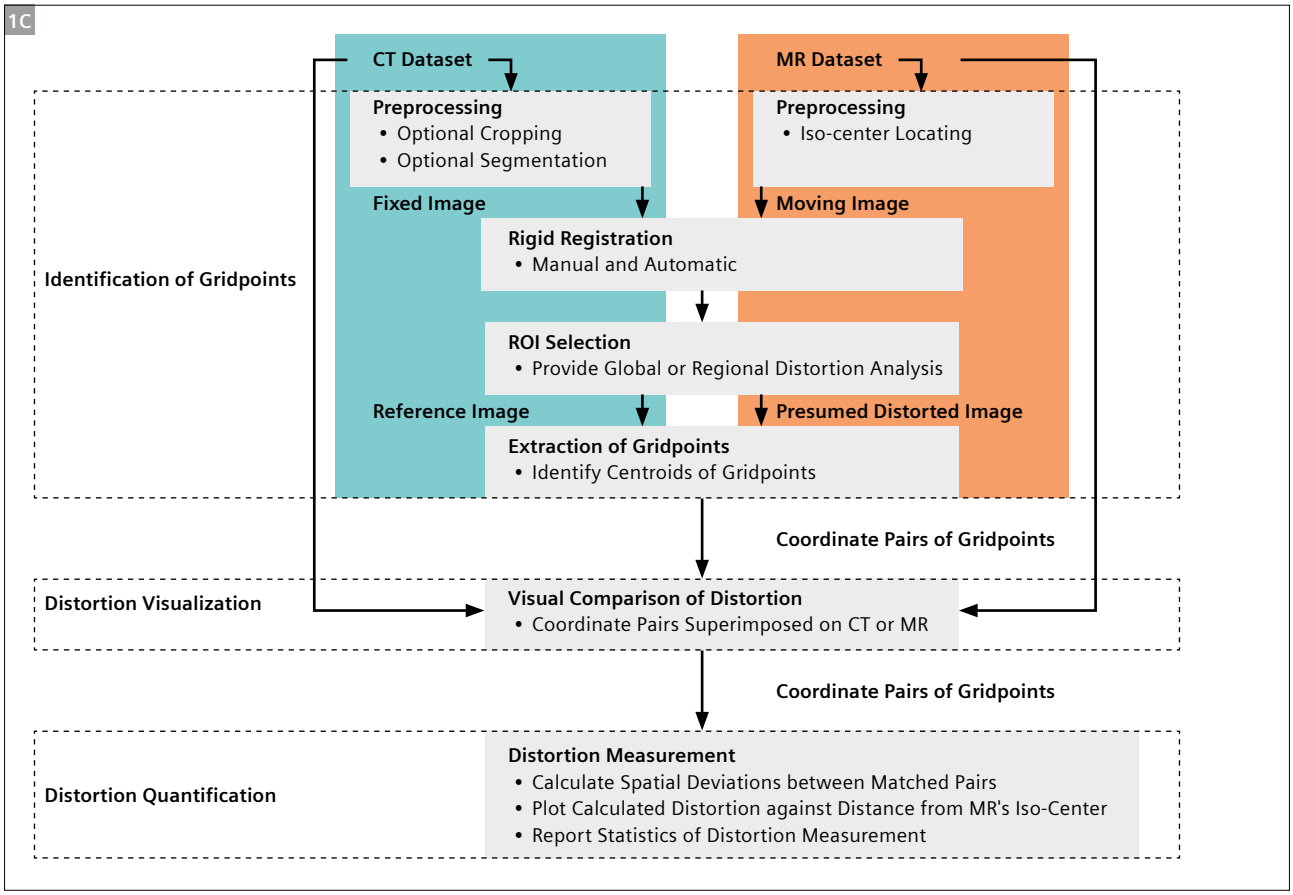


**1** **(1A)** User interface of the distortion measurement prototype with qualitative visualization; **(1B)** user interface with quantitative evaluation; **(1C)** backend pipeline of the distortion measurement prototype; **(1D)** the user interface matches the work and description in (1C), and was created with the intent of a user friendly design, with a straightforward step-by-step workflow.

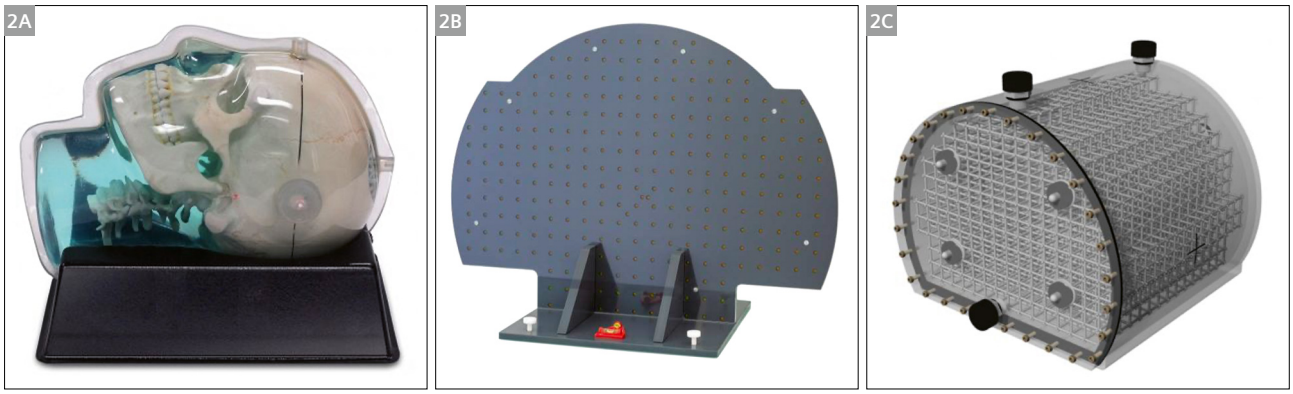


**2** **(2A)** Anthropomorphic skull phantom with a grid spacing of 15 mm and grid diameter of 3 mm (Model 603A, CIRS Inc.); **(2B)** generic large-field 2D phantom with a grid spacing of 30 mm and grid diameter of 5 mm (Siemens Healthcare); and **(2C)** generic large-bore 3D phantom with a grid spacing of 20 mm and grid diameter of 3 mm (Model 604, CIRS Inc.).

centres with limited resources. Most of the current software also requires the user to perform this type of analysis offline. Because of these limitations, we sought to provide a flexible solution where the user can bring their own "grid-like" phantoms (which could be 3D-printed in-house) and perform the analysis directly on the scanner, within the software ecosystem of the console. In this work, we developed a novel online distortion measurement prototype that can either be housed in the scanner's ecosystem, allowing an "on-the-fly" distortion assessment on the MR console, or operate offline on a personal computer (PC) for standalone analysis.

## Methods

The distortion measurement prototype was developed on the *syngo*.via Frontier platform (Siemens Healthcare, Erlangen, Germany). It can be integrated into the inline *syngo*.via MRI ecosystem from Siemens Healthcare, or it can operate offline as standalone software available on a Windows® system. The prototype requires a CT image of the phantom as a reference image. Acquired MR images are compared against the reference, and the software computes the distortion as a function of distance from isocentre. The prototype's user interface and backend processing pipeline are described in Figure 1, and the methods for extracting grid points are based on the approaches proposed by Stanescu et al. [21]. Three different types of distortion phantoms containing orthogonal grids of rods were used in this study to demonstrate the efficacy and versatility of the prototype. As shown in Figure 2, these phantoms include an anthropomorphic skull phantom (Model 603A, CIRS Inc., Norfolk, VA, USA), a generic large-field 2D phantom (Siemens Healthcare; note that LAP have a commercialized THETIS phantom developed on the basis of the prototype 2D phantom from Siemens Healthcare), and a generic large-bore 3D phantom (Model 604, CIRS Inc., Norfolk, VA, USA). To summarize the distortion, the prototype uses the extracted grid points from both CT and MR to provide not only an intuitive visual comparison but also a quantitative evaluation, including their calculated distortion deviations against the distance to isocenter with statistical information (i.e., minimum, maximum, and mean residual distortion). Lastly, the results can be saved locally by exporting the displayed data as a comma-separated values (CSV) file. The export file contains both scanner-specific information (field strength, gradient type, scanner make, etc.) and coordinates from the MR and CT datasets used for statistical analysis, which could be imported into quality assurance tracking programs.

## Results

Figures 3, 4, and 5 show the distortion assessments produced by the prototype for, respectively, the CIRS skull phantom, the 2D large-field phantom from Siemens Healthcare, and the CIRS large-bore phantom. Panel A in each of the figures shows the results of the automatic rigid image registration displayed at the slice near the isocenter. The CT (blue) and MRI (red) datasets are well matched. Panel B in each figure is the 3D rendering of the representations of the grid points' coordinate pairs (MRI: magenta, CT: green), providing an overall visualization of the spatial distortion for users. Panels C and D display the calculated coordinates positioned at the center of the grid points of the MR and CT images. Panels C and D also exhibit the qualitative spatial distortion between the acquired MR image compared to the reference CT image. Panel E summarizes a quantitative evaluation of the distortion measurement from MR for each phantom, including a distortion plot and statistical information.

## Discussion

The software prototype[1] requires, at a minimum, a reference CT image and a single MR image. By design, the software can analyze most types of grid-like phantoms, as demonstrated in this work. This allows users to 3D-print their own phantom for custom use cases. The rigid image registration is the first step to ensure the accuracy of distortion measurements since a potential inaccuracy in co-registration between two modalities will bring additional spatial deviations. In the prototype, we perform a manual registration followed by an auto-registration step to minimize the spatial discrepancy. Otherwise, the auto-registration might prioritize the minimization of the spatial variation resulting from the geometric distortion.

[1]*Work in progress. The application is currently under development and is not for sale in the U.S. and in other countries. Its future availability cannot be ensured.*

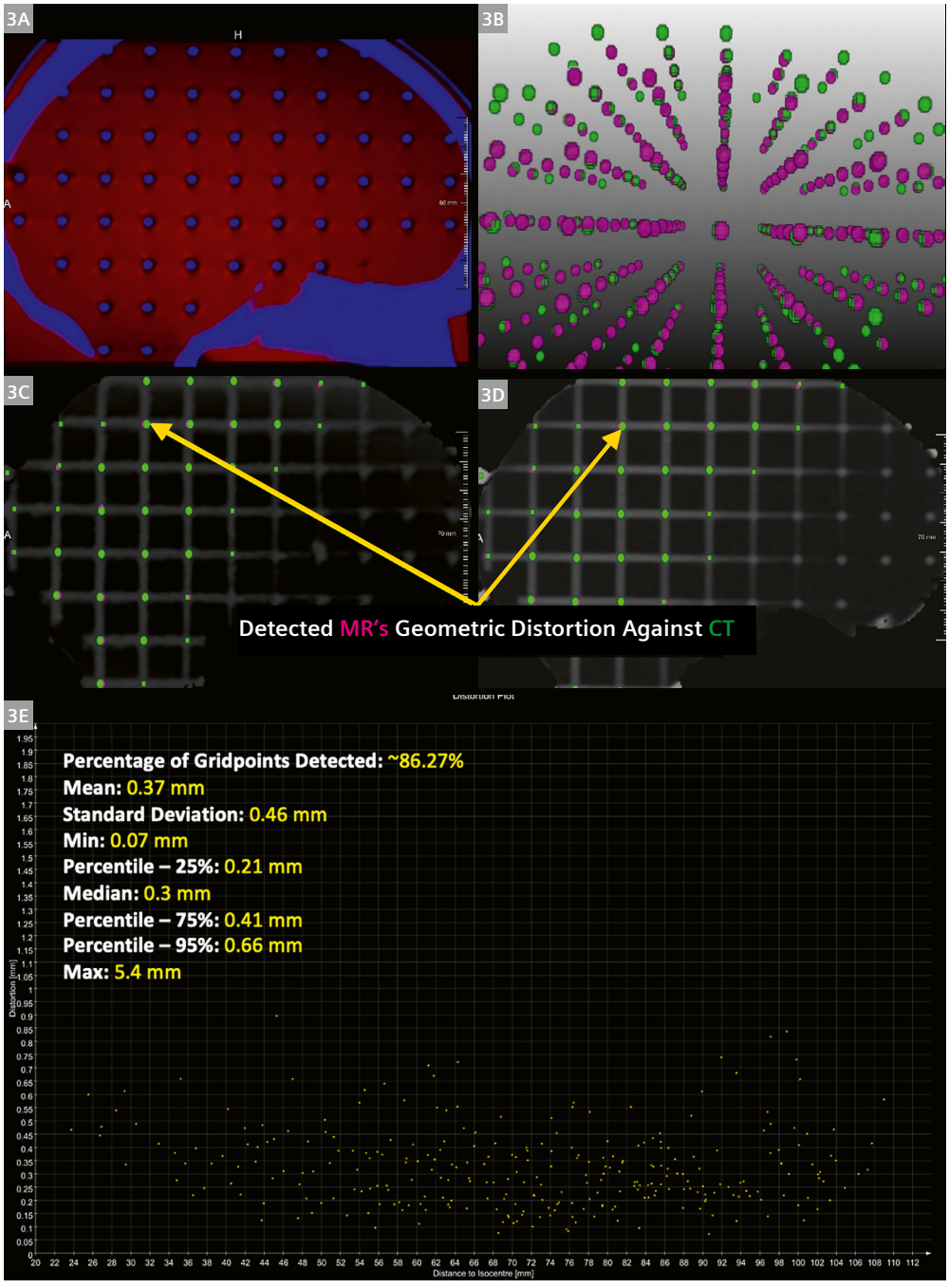


**3** Using the CIRS 603A, we present **(3A)** the results of rigid registration displayed at the slice near the isocenter (MR: red, CT: blue); **(3B)** 3D rendering of the representations of the grid points' coordinate pairs (MR: magenta, CT: green); **(3C)** coordinate pairs superimposed on MR image; **(3D)** coordinate pairs superimposed on CT image; and **(3E)** distortion plot against the distance from the isocenter.

Once the proper registration is visually verified, the extraction method can effectively detect the grid points for either MR (Figs. 3–5C) or CT (Figs. 3–5D) in each phantom, despite differences in contrast between MR and CT. The distortion can then be inspected slice by slice in an orthogonal view or a perspective 3D view. Sometimes, the points might be misidentified due to imaging artifacts. This issue can be easily addressed by acquiring CT and MR images with more homogenous intensity, finer contrast, and higher resolution. Lastly, for the distortion plot, the 2D large-field phantom and the 3D large-bore phantom suggest a trend of increasing spatial distortion

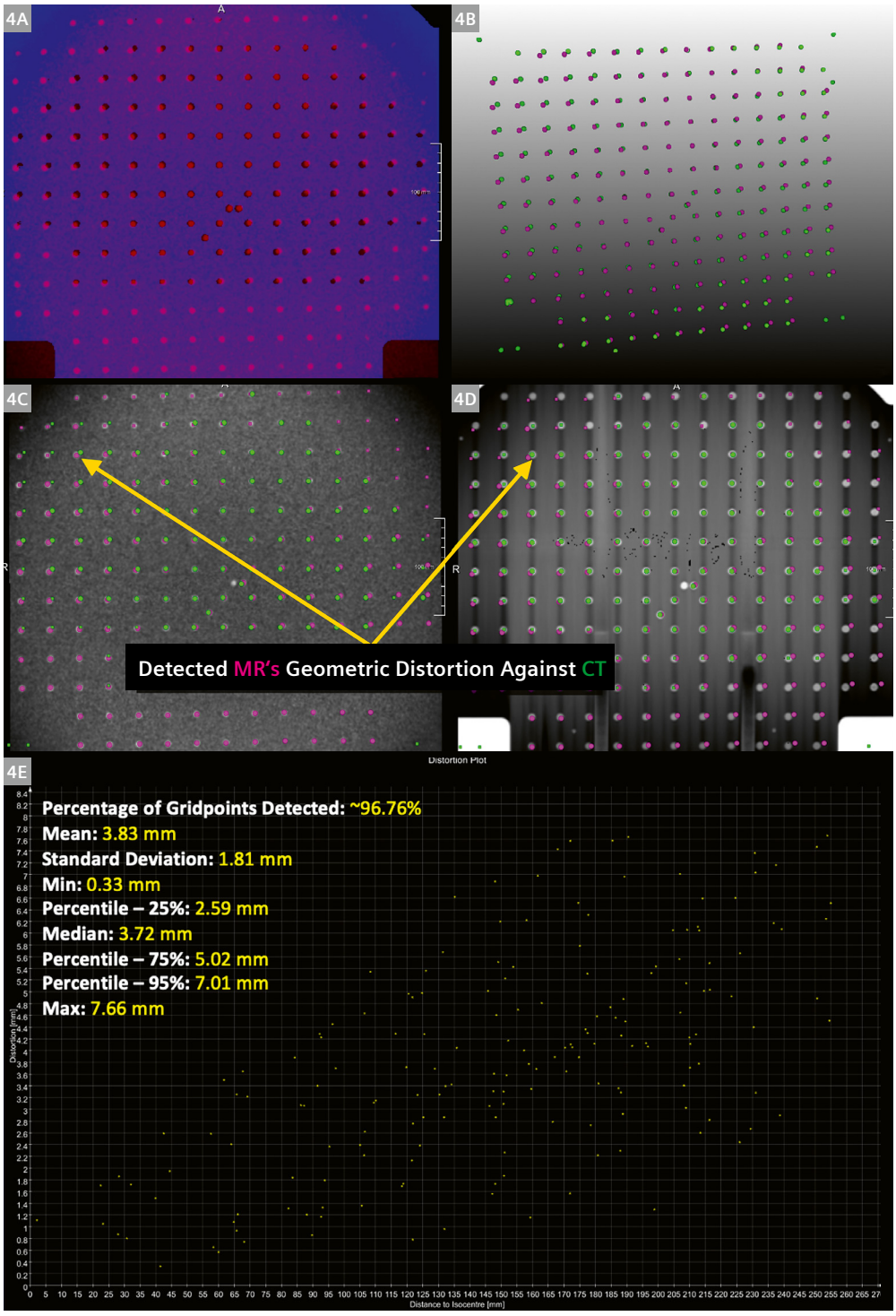


**4** Using the 2D large-field phantom from Siemens Healthcare, we present **(4A)** the results of rigid registration displayed at the slice near the isocenter (MR: red, CT: blue); **(4B)** 3D rendering of the representations of the grid points' coordinate pairs (MR: magenta, CT: green); **(4C)** coordinate pairs superimposed on MR image; **(4D)** coordinate pairs superimposed on CT image; and **(4E)** distortion plot against the distance from the isocenter.

with increasing distance from the isocenter, which corresponds to our expectations. On the other hand, the skull phantom did not show a similar upward trend because of the smaller field of view. In summary, achieving accurate spatial distortion measurements using our prototype relies on high-quality images, which can be achieved using optimized CT and MR protocols.

Please note that THETIS 3D MR Distortion Phantom test protocols are available on the MAGNETOM World Website in order to run QA tests: **https://www.magnetomworld.siemens-healthineers.com/clinical-corner/protocols/mr-in-rt/thetis-3d-mr-distortion-phantom-test**

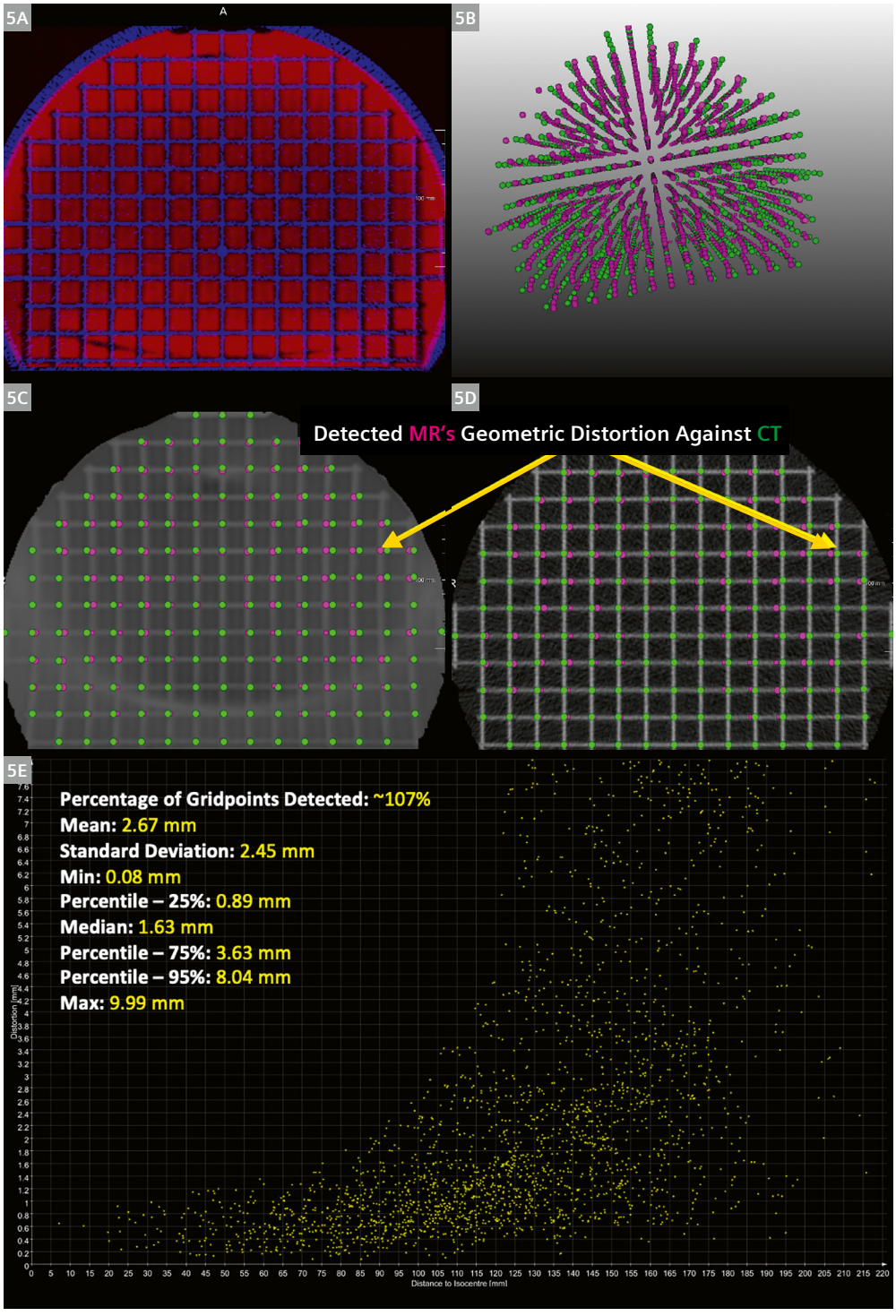


**5** Using the CIRS large-bore phantom, we present **(5A)** the results of rigid registration displayed at the slice near the isocenter (MR: red, CT: blue); **(5B)** 3D rendering of the representations of the grid points' coordinate pairs (MR: magenta, CT: green); **(5C)** coordinate pairs superimposed on MR image; **(5D)** coordinate pairs superimposed on CT image; and **(5E)** distortion plot against the distance from the isocenter.

## Conclusion

This work develops a novel online software prototype which can provide automatic vivid visualization and quantitative evaluation of spatial distortion for both small and large grid-like phantoms.

## Summary of main findings

The novelty of this work is the software prototype[1], which may be used as a standalone solution or run directly on the MR console. It can also be incorporated into the MR ecosystem, thus providing an online solution that users can easily access for routine quality assurance of MR images for radiation treatment planning.

[1]*Work in progress. The application is currently under development and is not for sale in the U.S. and in other countries. Its future availability cannot be ensured.*

### References


1 Schad LR, Ehricke HH, Wowra B, Layer G, Engenhart R, Kauczor HU, et al. Correction of spatial distortion in magnetic resonance angiography for radiosurgical treatment planning of cerebral arteriovenous malformations. Magn Reson Imaging. 1992;10(4):609–621.

2 Maurer CR Jr, Aboutanos GB, Dawant BM, Gadamsetty S, Margolin RA, Maciunas RJ, et al. Effect of geometrical distortion correction in MR on image registration accuracy. J Comput Assist Tomogr. 1996;20(4):666–679.

3 Moerland MA, Beersma R, Bhagwandien R, Wijrdeman HK, Bakker CJ. Analysis and correction of geometric distortions in 1.5 T magnetic resonance images for use in radiotherapy treatment planning. Phys Med Biol. 1995;40(10):1651–1654.

4 Kooy HM, van Herk M, Barnes PD, Alexander E 3rd, Dunbar SF, Tarbell NJ, et al. Image fusion for stereotactic radiotherapy and radiosurgery treatment planning. Int J Radiat Oncol Biol Phys. 1994;28(5):1229–1234.

5 Chomy F, Muyldermans P, Chemin A, Kind M, Thomas L, Le Treut AL, et al. [MRI and radiotherapy. External references, selection of plans and measurement of distortion]. Bull Cancer Radiother. 1994;81(3):241–246. French.

6 Hall WA, Paulson ES, van der Heide UA, Fuller CD, Raaymakers BW, Lagendijk JJW, et al. The transformation of radiation oncology using real-time magnetic resonance guidance: A review. Eur J Cancer. 2019;122:42–52.

7 Das IJ, McGee KP, Tyagi N, Wang H. Role and future of MRI in radiation oncology. Br J Radiol. 2019;92(1094):20180505.

8 Lagendijk JJ, Raaymakers BW, van Vulpen M. The magnetic resonance imaging-linac system. Semin Radiat Oncol. 2014 Jul;24(3):207–209.

9 Gao Y, Yoon S, Savjani R, Pham J, Kalbasi A, Raldow A, et al. Comparison and evaluation of distortion correction techniques on an MR-guided radiotherapy system. Med Phys. 2021;48(2):691–702.

10 Tadic T, Jaffray DA, Stanescu T. Harmonic analysis for the characterization and correction of geometric distortion in MRI. Med Phys. 2014;41(11):112303.

11 Wachowicz K, Stanescu T, Thomas SD, Fallone BG. Implications of tissue magnetic susceptibility-related distortion on the rotating magnet in an MR-linac design. Med Phys. 2010 Apr;37(4):1714–1721.

12 Crijns SP, Raaymakers BW, Lagendijk JJ. Real-time correction of magnetic field inhomogeneity-induced image distortions for MRI-guided conventional and proton radiotherapy. Phys Med Biol. 2011;56(1):289–297. Epub 2010 Dec 9.

13 Baldwin LN, Wachowicz K, Thomas SD, Rivest R, Fallone BG. Characterization, prediction, and correction of geometric distortion in 3 T MR images. Med Phys. 2007;34(2):388–399.

14 Sullivan TP, Harkenrider MM, Surucu M, Wood AM, Yacoub JH, Shea SM. Reduction of MRI signal distortion from titanium intracavitary brachytherapy applicator by optimizing pulse sequence parameters. Brachytherapy. 2018;17(2):377–382.

15 Han S, Yin FF, Cai J. Evaluation of dosimetric uncertainty caused by MR geometric distortion in MRI-based liver SBRT treatment planning. J Appl Clin Med Phys. 2019;20(2):43–50.

16 Stanescu T, Jaffray D. Investigation of the 4D composite MR image distortion field associated with tumor motion for MR-guided radiotherapy. Med Phys. 2016;43(3):1550–62.

17 Martin GV, Kudchadker RJ, Bruno TL, Frank SJ, Wang J. Comparison of prostate distortion by inflatable and rigid endorectal MRI coils in permanent prostate brachytherapy imaging. Brachytherapy. 2018;17(2):298–305.

18 Pappas EP, Seimenis I, Dellios D, Kollias G, Lampropoulos KI, Karaiskos P. Assessment of sequence dependent geometric distortion in contrast-enhanced MR images employed in stereotactic radiosurgery treatment planning. Phys Med Biol. 2018;63(13):135006.

19 Walker A, Metcalfe P, Liney G, Batumalai V, Dundas K, Glide-Hurst C, et al. MRI geometric distortion: Impact on tangential whole-breast IMRT. J Appl Clin Med Phys. 2016;17(5):7–19.

20 Jackson AS, Reinsberg SA, Sohaib SA, Charles-Edwards EM, Mangar SA, South CP, et al. Distortion-corrected T2 weighted MRI: a novel approach to prostate radiotherapy planning. Br J Radiol. 2007;80(959):926–933.

21 Stanescu T, Jans HS, Wachowicz K, Fallone BG. Investigation of a 3D system distortion correction method for MR images. J Appl Clin Med Phys. 2010;11(1):2961.


## Contact


Niranjan Venugopal, PhD, MSc, MCCPM
Medical Physicist, Department of Radiotherapy Physics
Assistant Professor, Department of Radiology, University of Manitoba
CancerCare Manitoba
675 McDermot Avenue
Winnipeg, R3E 0V9
Canada
Tel.: +1 204-787-1737
nvenugopal@cancercare.mb.ca


Niranjan Venugopal, PhD, MSc

Gerald Moran, Ph.D.

Lumeng Cui, Ph.D.